Computational Mechanics (1990) 6, 379–391

Computational Mechanics

On the three-dimensional stress field around a circular hole in a plate of arbitrary thickness

E. S. Folias and **J.-J. Wang**
Department of Mechanical Engineering, University of Utah, Salt Lake City, UT 84112, USA

Abstract. An analytical solution for the three-dimensional stress field in a plate of an arbitrary thickness, $2h$, and weakened by a cylindrical hole of radius a is presented. Far away from the hole, the plate is subjected to a uniform tensile load, σ_0, in a direction parallel to the plane of the plate. The solution is shown to be derivable from a general $3D$ solution, which the first author constructed in a previous paper. The analysis shows the stress concentration factor to vary across the thickness and to be sensitive to the value of the radius to thickness ratio, a/h. Furthermore, it is shown that for ratios of $(a/h) \geqq 4$, the results predicted by plane stress theory are more than adequate for engineering applications. Finally, the transition between plane stress and plane strain appears to occur at $a/h = 0.5$.

1 Introduction

It is well known that corner cracks at holes are among the most common flaws in aircraft structures (Fig. 1). In one case history, e.g., a certain aluminum alloy was chosen for the wing skin of a military aircraft because of its high strength and light weight ratio. Moreover, the design stress on the wing was set at a high level to increase the aircraft's payload capacity. Inevitably, a fatigue crack grew out from a rivet hole, in one of the aluminum wing plates, and progressed to the point where catastrophic failure took place. What was most unfortunate about this particular failure was the fact that the allowable flaw size that could be tolerated by the material under the applied stress was smaller than the diameter of the rivet head covering the hole. As a result, it was impossible for maintenance and inspection crews to know that the crack was growing from the rivet hole until it was too late. While this catastrophic failure could have been avoided in several ways, the best design philosophy would have been to take appropriate measures so that no crack, however, small, would manifest itself.

Experimental evidence shows that for relatively thin plates the crack either originates at the corner[1], where the hole meets the free surface of the plate, or at the center of the plate. On the other hand for relatively thick plates the crack almost always originates in the vicinity of the corner (Broek 1974). Of course, cracks in general originate from small imperfections or discontinuities that may be present in the material. Such discontinuities may either be man-made or may be introduced in the material during the process of fabrication.

Thus, one possible explanation for this phenomenon is that such discontinuities are most likely to be present in the vicinity where the hole meets the free surface of the plate. Another possible explanation could be that at such neighborhoods the stress levels may actually be higher than those predicted by the two-dimensional elasticity theory, i.e., the usual stress concentration factor of 3.

This problem, of course, has been studied by several researchers. At first, due to the difficulty posed by three-dimensional elasticity problems, most analytical studies were based on two-dimensional linear theory of homogeneous and isotropic materials. In 1898, the $2D$ solution for the case of a single circular hole in an infinite plate was obtained by Kirsch (1898). Problems

[1] Comment refers to an in-plane tensile load

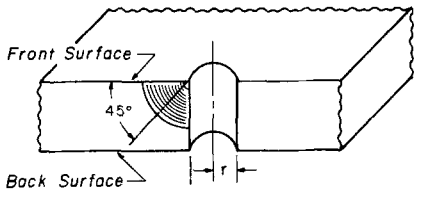

Fig. 1. Circular corner crack at a fastener hole

dealing with finite-plate dimensions, multiple holes and different shapes of holes were solved by Muskhelishvili (1953). Most of this work was accomplished by means of conformal mapping techniques. Comprehensive reviews on this subject have been given by Neuber (1985) and Savin (1961). However, in the case where the diameter of the hole $2a$ is of the same order of magnitude as the thickness $2h$ of the plate ($|z| \leqq h$), these two-dimensional solutions can no longer provide accurate approximation due to the very "thin" or very "thick" assumptions.

In order to obtain a more general solution to the stress concentration problem, studies on the three-dimensional theory of elasticity become essential. It was not until 1948 that Green (1948) developed a formal $3D$ solution which was in an infinite series form. Unfortunately, he did not have access to modern computing facilities and as a result the numerical work is limited to the case where $(a/h) = 1$. The work, however, opened up new areas for further research.

An approximate solution to the problem was given in 1949 by Sternberg and Sadowsky (1949). Their approach was a modified version of the Ritz method. Specifically, a z-dependence of the form

$$\left[\left(\frac{z}{h}\right)^n - 1\right]^2, \tag{1}$$

and a θ-dependence of the form $e^{i2\theta}$, were assumed (r, θ polar coordinates in the plane of the plate). The stress field was, subsequently, substituted into the strain energy which was then minimized to give the functional dependence in r.

Subsequently, in 1957, Alblas (1957) using the same solution proposed by Green (1949) extended the numerical results to also include other ratios of practical interest. In order to satisfy the boundary conditions at the hole, he reduced the problem to that of the solution of an infinite system of equations for the unknown complex coefficients. The system was subsequently truncated and its solution was sought numerically. The results are given in Fig. 2 where it is shown that the stress concentration factor attains a maximum at the center of the plate and that it decreases parabolically as one approaches the free surfaces of the plate.

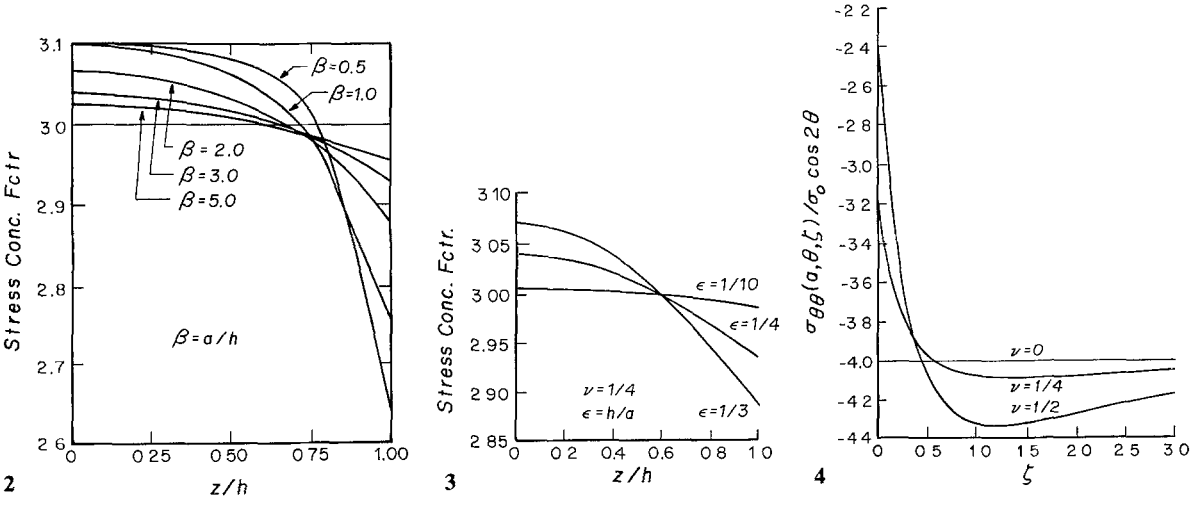

Figs. 2–4. Stress concentration factor across the thickness for Poisson's ratio $\nu = 0.25$ and various a/h ratios **2** (Alblas 1957); **3** (Reiss 1962). **4** Stress concentration factor as a function of the depth $\zeta = \frac{z}{a}$. (Youngdahl and Sternberg 1966). ν = Poisson's ratio

In 1962, Reiss (1963) using a perturbation analysis was able to obtain a solution which yielded "three-dimensional" corrections to those of the generalized plane stress. The problem was ultimately reduced to a series form where an approximation was introduced in order to obtain numerical results. The results which are valid for small values of thickness to diameter ratios, substantiate the findings by Alblas and are shown in Fig. 3.

In Alblas (1957) and Reiss (1963) it appears that the focus of the investigation has been on diameter to thickness ratios greater than or equal to 0.5. The authors suspect that this was due to the enormous numerical difficulties that this problem presents. Be that as it may, their results showed the stress concentration factor to attain its maximum in the middle of the plate and to decrease parabolically as one approaches the, free of stress, plate surfaces.

This trend, however, does not seem to explain the experimental observations that for thin plates fatigue cracks either develop at the corner, i.e., where the hole meets the free surface, or at the center of the plate. On the other hand, for relatively thick plates the crack almost always appears at the corner. Moreover, there exists no precise definition as to what constitutes a thin or a thick plate. For this reason Youngdahl and Sternberg (1966) investigated the stress field in an elastic half-space with a semi-infinite transverse circular cylindrical hole. The problem was finally formulated as a Fredholm integral equation of the second kind, the solution of which was sought numerically. Their results showed that all of the three-dimensional effects were highly sensitive to changes in Poisson's ratio and became more pronounced at larger values of this parameter. Furthermore they discovered the presence of a stress boundary layer in the vicinity of the free surfaces (Fig. 4).

The purpose of this paper is three-fold. First to show that the solution of the cylindrical hole problem is derivable from the same general analytical solution from which the $3D$ crack problem can be derived. Second to acquire enough experience and a "feel" for the ultimate construction of an explicit analytical solution to the crack problem. Third to show that the two existing asymptotic solutions can be extracted from the same analysis, bridging, therefore, the gap between "thin" and "thick" plates.

2 Formulation of the problem

Consider the equilibrium of a homogeneous, isotropic, elastic plate which occupies the space $|x| < \infty, |z| \leqq h$ and contains a cylindrical hole of radius a whose generators are perpendicular to the bounding planes, namely, $z = \pm h$. Let the plate be subjected to a uniform tensile load σ_0 along the y-axis and parallel to the bounding planes (Fig. 5).

In the absence of body forces, the coupled differential equations governing the displacement

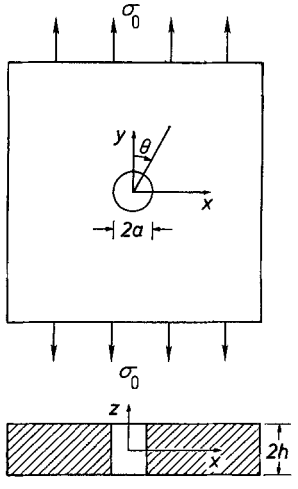

Fig. 5. Geometrical configuration of a plate weakened by a circular hole of radius a

functions u, v and w are:

$$\frac{m}{m-2}\frac{\partial e}{\partial x}+\nabla^2 u=0 \tag{2}$$

$$\frac{m}{m-2}\frac{\partial e}{\partial y}+\nabla^2 v=0 \tag{3}$$

$$\frac{m}{m-2}\frac{\partial e}{\partial z}+\nabla^2 w=0, \tag{4}$$

where $\nabla^2 \equiv (\partial^2/\partial x^2)+(\partial^2/\partial y^2)+(\partial^2/\partial z^2)$ is the Laplacian operator, $m \equiv 1/v$, v is Poisson's ratio, and

$$e \equiv \frac{\partial u}{\partial x}+\frac{\partial v}{\partial y}+\frac{\partial w}{\partial z}. \tag{5}$$

The stress-displacement relations are given by Hooke's law as

$$\sigma_{xx}=2G\left(\frac{\partial u}{\partial x}+\frac{e}{m-2}\right), \quad \sigma_{yy}=2G\left(\frac{\partial v}{\partial y}+\frac{e}{m-2}\right), \quad \sigma_{zz}=2G\left(\frac{\partial w}{\partial z}+\frac{e}{m-2}\right) \tag{6–8}$$

$$\tau_{xy}=G\left(\frac{\partial u}{\partial y}+\frac{\partial v}{\partial x}\right), \quad \tau_{yz}=G\left(\frac{\partial v}{\partial z}+\frac{\partial w}{\partial y}\right), \quad \tau_{zx}=G\left(\frac{\partial w}{\partial x}+\frac{\partial u}{\partial z}\right), \tag{9–11}$$

with G being the shear modulus of the plate.

As to the boundary conditions, one must require that

$$\text{as} \quad |x|\to\infty : \sigma_{xx}=\tau_{xy}=\tau_{xz}=0 \tag{12}$$

$$\text{as} \quad |y|\to\infty : \tau_{xy}=\tau_{yz}=0, \quad \sigma_{yy}=\sigma_0 \tag{13}$$

$$\text{at} \quad |z|=h : \tau_{xz}=\tau_{yz}=\sigma_{zz}=0 \tag{14}$$

$$\text{at} \quad r=a : \sigma_{rr}=\tau_{r\theta}=\tau_{rz}=0. \tag{15}$$

It is found convenient to seek the solution of the problem in the form

$$u=u^{(P)}+u^{(c)}, \text{etc.}, \tag{16}$$

where the first component represents the usual "undisturbed" or "particular" solution of a plate without the presence of a hole. Such a particular solution can easily be constructed and for the problem at hand is:

$$u^{(P)}=-\frac{\sigma_0}{2G\Delta}(m-2)^2 x \tag{17}$$

$$v^{(P)}=-[1-(m-1)^2]\frac{\sigma_0(m-2)}{2G\Delta}y \tag{18}$$

$$w^{(P)}=-(m-2)^2\frac{\sigma_0}{2G\Delta}z, \tag{19}$$

where

$$\Delta \equiv (m+1)(m-2)^2. \tag{20}$$

By using Hooke's law and the appropriate coordinate transformation, one can find the stress field due to the particular solution to be of the form

$$\sigma_{rr}^{(P)}=\tfrac{1}{2}\sigma_0[1+\cos(2\theta)], \quad \sigma_{\theta\theta}^{(P)}=\tfrac{1}{2}\sigma_0[1-\cos(2\theta)], \quad \tau_{r\theta}^{(P)}=-\tfrac{1}{2}\sigma_0\sin(2\theta). \tag{21–23}$$

3 Mathematical statement of the complementary problem

In review of the particular solution, one needs to find three functions: $u^{(c)}(x, y, z), v^{(c)}(x, y, z)$ and $w^{(c)}(x, y, z)$, such that they satisfy the partial differential Eqs. (2–4) and the following boundary conditions:

$$\text{at} \quad |z| = h: \sigma_{zz}^{(c)} = \tau_{xz}^{(c)} = \tau_{yz}^{(c)} = 0 \tag{24}$$

$$\text{at} \quad r = a: \sigma_{rr}^{(c)} = -\sigma_{rr}^{(P)}, \quad \tau_{r\theta}^{(c)} = -\tau_{r\theta}^{(P)}, \quad \tau_{rz}^{(c)} = -\tau_{rz}^{(P)}. \tag{25–27}$$

Finally, in order to complete the formulation of the problem, one must also require that all the complementary displacements and the complementary stresses do vanish as $r \to \infty$.

4 Method of solution

A general three-dimensional solution to Navier's equation for plates of uniform thickness, $2h$, and with plate faces free of stress has previously been constructed by the first author and the results are reported in Folias (1975). Perhaps it may be appropriate here to note that the same displacement field is also recovered if one uses a double Fourier integral transform in x and y and the subsequent use of a contour integration. This matter is discussed in great detail in Wilcox (1978)[2]. Without going into the mathematical details, the complementary displacement and stress fields are[3]:

(i) the displacement field:

$$\begin{aligned} u^{(c)} = {} & \frac{1}{m-2} \sum_{\nu=1}^{\infty} A_\nu \frac{\partial H_\nu}{\partial x} \{2(m-1)\cos(\beta_\nu h)\cos(\beta_\nu z) \\ & + m\beta_\nu h \sin(\beta_\nu h)\cos(\beta_\nu z) - m\beta_\nu z \cos(\beta_\nu h)\sin(\beta_\nu z)\} \\ & + \sum_{n=1}^{\infty} B_n \frac{\partial H_n^*}{\partial y} \cos(\alpha_n h)\cos(\alpha_n z) + I_1 - y\frac{\partial I_3}{\partial x} + \frac{1}{m+1} z^2 \frac{\partial^2 I_3}{\partial x \partial y}. \end{aligned} \tag{28}$$

$$\begin{aligned} v^{(c)} = {} & \frac{1}{m-2} \sum_{\nu=1}^{\infty} A_\nu \frac{\partial H_\nu}{\partial y} \{2(m-1)\cos(\beta_\nu h)\cos(\beta_\nu z) \\ & + m\beta_\nu h \sin(\beta_\nu h)\cos(\beta_\nu z) - m\beta_\nu z \cos(\beta_\nu h)\sin(\beta_\nu z)\} \\ & - \sum_{n=1}^{\infty} B_n \frac{\partial H_n^*}{\partial x} \cos(\alpha_n h)\cos(\alpha_n z) + \frac{3m-1}{m+1} I_3 + I_2 - y\frac{\partial I_3}{\partial y} - \frac{1}{m+1} z^2 \frac{\partial^2 I_3}{\partial x^2}. \end{aligned} \tag{29}$$

$$\begin{aligned} w^{(c)} = {} & \frac{1}{m-2} \sum_{\nu=1}^{\infty} A_\nu H_\nu \beta_\nu \{(m-2)\cos(\beta_\nu h)\sin(\beta_\nu z) \\ & - m\beta_\nu h \sin(\beta_\nu h)\sin(\beta_\nu z) - m\beta_\nu z \cos(\beta_\nu h)\cos(\beta_\nu z)\} - \frac{2}{m+1} z \frac{\partial I_3}{\partial y}. \end{aligned} \tag{30}$$

(ii) the stress field:

$$\begin{aligned} \frac{1}{2G}\sigma_{xx}^{(c)} = {} & \frac{2}{m-2} \sum_{\nu=1}^{\infty} A_\nu \beta_\nu^2 H_\nu \cos(\beta_\nu h)\cos(\beta_\nu z) \\ & + \frac{1}{m-2} \sum_{\nu=1}^{\infty} A_\nu \frac{\partial^2 H_\nu}{\partial x^2} \{2(m-1)\cos(\beta_\nu h)\cos(\beta_\nu z) \end{aligned}$$

[2] Folias, independently also investigated this matter in 1977

[3] Due to symmetry, we assume $y \geqq 0$

$$+ m\beta_v h \sin(\beta_v h)\cos(\beta_v z) - m\beta_v z \cos(\beta_v h)\sin(\beta_v z)\}$$
$$+ \sum_{n=1}^{\infty} B_n \frac{\partial^2 H_n^*}{\partial x \partial y}\cos(\alpha_n h)\cos(\alpha_n z) + \frac{\partial I_1}{\partial x} - y\frac{\partial^2 I_3}{\partial x^2} + \frac{1}{m+1} z^2 \frac{\partial^3 I_3}{\partial x^2 \partial y} + \frac{2}{m+1}\frac{\partial I_3}{\partial y}. \tag{31}$$

$$\frac{1}{2G}\sigma_{yy}^{(c)} = \frac{2}{m-2}\sum_{v=1}^{\infty} \beta_v^2 A_v H_v \cos(\beta_v h)\cos(\beta_v z)$$
$$- \frac{1}{m-2}\sum_{v=1}^{\infty} A_v \left\{\frac{\partial^2 H_v}{\partial x^2} - \beta_v^2 H_v\right\}\{2(m-1)\cos(\beta_v h)\cos(\beta_v z)$$
$$+ m\beta_v h \sin(\beta_v h)\cos(\beta_v z) - m\beta_v z \cos(\beta_v h)\sin(\beta_v z)\}$$
$$- \sum_{n=1}^{\infty} B_n \frac{\partial^2 H_n^*}{\partial x \partial y}\cos(\alpha_n h)\cos(\alpha_n z) + \frac{2m}{m+1}\frac{\partial I_3}{\partial y} - \frac{\partial I_1}{\partial x} + y\frac{\partial^2 I_3}{\partial x^2} - \frac{1}{m+1} z^2 \frac{\partial^3 I_3}{\partial x^2 \partial y}. \tag{32}$$

$$\frac{1}{2G}\sigma_{zz}^{(c)} = \frac{m}{m-2}\sum_{v=1}^{\infty} A_v H_v \beta_v^2 \{-\beta_v h \sin(\beta_v h)\cos(\beta_v z) + \beta_v z \cos(\beta_v h)\sin(\beta_v z)\}. \tag{33}$$

$$\frac{1}{G}\tau_{xy}^{(c)} = \frac{2}{m-2}\sum_{v=1}^{\infty} A_v \frac{\partial^2 H_v}{\partial x \partial y}\{2(m-1)\cos(\beta_v h)\cos(\beta_v z)$$
$$+ m\beta_v h \sin(\beta_v h)\cos(\beta_v z) - m\beta_v z \cos(\beta_v h)\sin(\beta_v z)\}$$
$$- \sum_{n=1}^{\infty} B_n \left\{2\frac{\partial^2 H_n^*}{\partial x^2} - \alpha_n^2 H_n^*\right\}\cos(\alpha_n h)\cos(\alpha_n z)$$
$$+ 2\left(\frac{m-1}{m+1}\right)\frac{\partial I_3}{\partial x} + 2\frac{\partial I_2}{\partial x} - \frac{2}{m+1} z^2 \frac{\partial^3 I_3}{\partial x^3} - 2y\frac{\partial^2 I_3}{\partial x \partial y}. \tag{34}$$

$$\frac{1}{G}\tau_{xz}^{(c)} = -\frac{2m}{m-2}\sum_{v=1}^{\infty} A_v \frac{\partial H_v}{\partial x}\beta_v\{\cos(\beta_v h)\sin(\beta_v z)$$
$$+ \beta_v h \sin(\beta_v h)\sin(\beta_v z) + \beta_v z \cos(\beta_v h)\cos(\beta_v z)\}$$
$$- \sum_{n=1}^{\infty} B_n \frac{\partial H_n^*}{\partial y}\alpha_n \cos(\alpha_n h)\sin(\alpha_n z) \tag{35}$$

$$\frac{1}{G}\tau_{yz}^{(c)} = -\frac{2m}{m-2}\sum_{v=1}^{\infty} A_v \beta_v \frac{\partial H_v}{\partial y}\{\cos(\beta_v h)\sin(\beta_v z)$$
$$+ \beta_v h \sin(\beta_v h)\sin(\beta_v z) + \beta_v z \cos(\beta_v h)\cos(\beta_v z)\}$$
$$+ \sum_{n=1}^{\infty} B_n \alpha_n \frac{\partial H_n^*}{\partial x}\cos(\alpha_n h)\sin(\alpha_n z), \tag{36}$$

where in order to express the solution in a more convenient form, we have adopted the following definitions[4]:

$$A_v \times H_v(x, y; \beta) = \int_0^{\infty} \frac{\Gamma_v}{s}\frac{e^{-\sqrt{s^2+\beta_v^2}|y|}}{\sqrt{s^2+\beta_v^2}}\cos(sx)\,ds, \tag{37}$$

$$(-1)^n B_n H_n^*(x, y; \alpha_n) = \int_0^{\infty} \frac{sS_n}{\sqrt{s^2+\alpha_n^2}}\frac{e^{-\sqrt{s^2+\alpha_n^2}|y|}}{\sqrt{s^2+\alpha_n^2}}\cos(sx)\,dx, \tag{38}$$

with A_v and B_n as constants but functions of β_v and a_n, respectively,

$$\alpha_n \equiv \frac{n\pi}{h} \quad n = 1, 2, 3, \ldots, \tag{39}$$

[4] Due to symmetry, in the case of the hole problem one need only to consider the first quadrant

β_ν are the roots of the transcendental equation

$$\sin(2\beta_\nu h) = -2(\beta_\nu h), \tag{40}$$

and[5]

$$I_1 = \int_0^\infty P(s)e^{-s|y|}\sin(sx)\,ds, \quad I_2 = \int_0^\infty P(s)e^{-s|y|}\cos(sx)\,ds, \quad I_3 = \int_0^\infty \frac{Q(s)}{s}e^{-s|y|}\cos(sx)\,ds. \tag{41–43}$$

It is an easy matter now to verify that the above displacement field does indeed satisfy Navier's equations and that the stresses $\sigma_{zz}^{(c)}, \tau_{xz}^{(c)}$ and $\tau_{yz}^{(c)}$ do vanish at the plate faces. Moreover, the displacements do vanish as $r \to \infty$ and the functions H_n and H_n^* satisfy the following differential equations:

$$\frac{\partial^2 H_\nu}{\partial x^2} + \frac{\partial^2 H_\nu}{\partial y^2} - \beta_\nu^2 H_\nu = 0, \quad \frac{\partial^2 H_n^*}{\partial x^2} + \frac{\partial^2 H_n^*}{\partial y^2} - \alpha_n^2 H_n^* = 0. \tag{44,45}$$

As a practical matter, by constructing appropriate solutions to the simplified differential Eqs. (44) and (45), one can now solve a whole class of $3D$ linear elastic problems, e.g., the problem of a cylindrical hole, an elliptical hole, a crack, a cylindrical inclusion, etc.

For the cylindrical hole problem for example, guided by the boundary conditions at the surface of the hole, i.e., at $r = a$

$$\sigma_{rr}^{(c)} = -(\sigma_0/2)[1 + \cos(2\theta)], \quad \tau_{r\theta}^{(c)} = (\sigma_0/2)\sin(2\theta), \quad \tau_{rz}^{(c)} = 0, \tag{46–48}$$

and utilizing the local coordinates, i.e.,

$$\sigma_{rr}^{(c)} = \sin^2(\theta)\sigma_{xx}^{(c)} + \cos^2(\theta)\sigma_{yy}^{(c)} + \sin(2\theta)\tau_{xy}^{(c)} \tag{49}$$

$$\tau_{r\theta}^{(c)} = \tfrac{1}{2}\sin(2\theta)\sigma_{xx}^{(c)} - \tfrac{1}{2}\sin(2\theta)\sigma_{yy}^{(c)} + \cos(2\theta)\tau_{xy}^{(c)} \tag{50}$$

$$\sigma_{rz}^{(c)} = \cos(\theta)\tau_{yz}^{(c)} + \sin(\theta)\tau_{xz}^{(c)}, \tag{51}$$

arrives at the conclusion that[6]

$$H_\nu = \frac{K_2(\beta_\nu r)}{\beta_\nu^2}\cos(2\theta), \quad H_n^* = \frac{K_2(\alpha_n r)}{\alpha_n^2}\sin(2\theta), \tag{52,53}$$

$$4GI_1 = \frac{\partial\phi}{\partial x}, \quad 4GI_2 = \frac{\partial\phi}{\partial y}, \quad 2GI_3 = \sigma_0 a^2 \frac{y}{x^2 + y^2} \tag{54–56}$$

with

$$\phi = \sigma_0 a^2 \left\{ \frac{\nu - 3}{1 + \nu}\ln r + \left[\frac{1}{2} + \frac{2\nu}{3(1+\nu)}\left(\frac{h}{a}\right)^2 - \frac{2\nu G}{(1-2\nu)\sigma_0} \sum_{\nu=1}^{\infty} A_\nu K_2(\beta_\nu a)\left[\frac{1}{\beta_\nu a}\frac{K_1(\beta_\nu a)}{K_2(\beta_\nu a)} + \frac{6}{\beta_\nu^2 a^2} \right] \right] \frac{a^2}{r^2}\cos(2\theta) \right\}. \tag{57}$$

Thus the boundary conditions at the surface of the hole, i.e. Eqs. (46–48), become respectively[7]:

$$\frac{2}{m-2}\sum_{\nu=1}^{\infty} A_\nu K_2(\beta_\nu a)\cos(\beta_\nu h)\cos(\beta_\nu z) + \frac{1}{m-2}\sum_{\nu=1}^{\infty} A_\nu \frac{\partial^2 K_2(\beta_\nu a)}{\partial(\beta_\nu a)^2}$$
$$\times \{2(m-1)\cos(\beta_\nu h)\cos(\beta_\nu z) + m\beta_\nu h\sin(\beta_\nu h)\cos(\beta_\nu z) - m\beta_\nu z\cos(\beta_\nu h)\sin(\beta_\nu z)\}$$

[5] The reader should notice that I_1, I_2, and I_3 are $2D$ harmonic functions

[6] The second solution, $I_2(\beta_\nu r)$, must be discarded for the displacement and stresses must be finite far away from the hole

[7] The reader should realize that Eqs. (58–60) do not necessarily need to be satisfied at $z = \pm h$. The problem may very well possess a stress singularity at such points and as a result one does not want to be too restrictive. The only admissible physical requirement which must be imposed is that at every point in the body the local strain energy must be finite. This matter is discussed in Wilcox (1979) and will also be investigated in Sect. 6

$$+\sum_{n=1}^{\infty} B_n\left\{-\frac{2}{\alpha_n a}\frac{\partial K_2(\alpha_n a)}{\partial(\alpha_n a)}+\frac{2}{(\alpha_n a)^2}K_2(\alpha_n a)\right\}\cos(\alpha_n h)\cos(\alpha_n z)$$

$$=\frac{3\sigma_0}{(m+1)G}\left(\frac{z}{a}\right)^2-C;\quad |z|\leqq h. \tag{58}$$

$$\frac{1}{m-2}\sum_{\nu=1}^{\infty} A_\nu\left\{-\frac{2}{\beta_\nu a}\frac{\partial K_2(\beta_\nu a)}{\partial(\beta_\nu a)^2}+\frac{2}{(\beta_\nu a)^2}K_2(\beta_\nu a)\right\}$$

$$\times\{2(m-1)\cos(\beta_\nu h)\cos(\beta_\nu z)+m\beta_\nu h\sin(\beta_\nu h)\cos(\beta_\nu z)-m\beta_\nu z\cos(\beta_\nu h)\sin(\beta_\nu z)\}$$

$$+\sum_{n=1}^{\infty} B_n\left\{\frac{\partial^2 K_2(\alpha_n a)}{\partial(\alpha_n a)^2}-\tfrac{1}{2}K_2(\alpha_n a)\right\}\times\cos(\alpha_n h)\cos(\alpha_n z)$$

$$=\frac{3\sigma_0}{(m+1)G}\left(\frac{z}{a}\right)^2-C;\quad |z|\leqq h \tag{59}$$

and

$$\frac{m}{m-2}\sum_{\nu=1}^{\infty} A_\nu\frac{\partial K_2(\beta_\nu a)}{\partial(\beta_\nu a)}\{\cos(\beta_\nu h)\sin(\beta_\nu z)+\beta_\nu h\sin(\beta_\nu h)\sin(\beta_\nu z)+\beta_\nu z\cos(\beta_\nu h)\cos(\beta_\nu z)\}$$

$$-\sum_{n=1}^{\infty} B_n\frac{1}{(\alpha_n a)}K_2(\alpha_n a)\cos(\alpha_n h)\sin(\alpha_n z)=0;\quad |z|\leqq h, \tag{60}$$

and

$$C\equiv\frac{\nu\sigma_0}{(1+\nu)G}\left(\frac{h}{a}\right)^2-\frac{3\nu}{1-2\nu}\sum_{\nu=1}^{\infty} A_\nu K_2(\beta_\nu a)\left[\frac{1}{\beta_\nu a}\frac{K_1(\beta_\nu a)}{K_2(\beta_\nu a)}+\frac{6}{(\beta_\nu a)^2}\right]. \tag{61}$$

It is interesting to note that the θ-dependence has now been eliminated and that it finally remains to solve the three equations for the unknown complex coefficients A_ν, and for the unknown real coefficients B_n. In order to accomplish this, we use the method discussed in Kantorovich and Krylov (1964). Specifically, we expand the functions $\cos(\beta_\nu z)$ and $(\beta_\nu z)\sin(\beta_\nu z)$ in terms of $\cos(\alpha_n z)$ and then equate terms. It should be noted that the system is extremely sensitive to even small changes of the coefficients. As a result, the methods of "collocation" and "least squares" lead to a nonconvergent solution. The aforementioned method, however furnishes us with coefficients that do converge as the number of roots used increases.

Once the unknown coefficients have been established, the stress $\sigma_{\theta\theta}$ may then be computed at any point in the body. Specifically,

$$\frac{1}{2G}\sigma_{\theta\theta}^{(c)}|_{\substack{r=a\\ \theta=\pi/2}}=-\frac{2}{m-2}\sum_{\nu=1}^{\infty} A_\nu K_2(\beta_\nu a)\cos(\beta_\nu h)\cos(\beta_\nu z)$$

$$+\frac{1}{m-2}\sum_{\nu=1}^{\infty} A_\nu\left\{\frac{\partial^2 K_2(\beta_\nu a)}{\partial(\beta_\nu a)^2}-K_2(\beta_\nu a)\right\}$$

$$\times\{2(m-1)\cos(\beta_\nu h)\cos(\beta_\nu z)+m\beta_\nu h\sin(\beta_\nu h)\cos(\beta_\nu z)-m\beta_\nu z\cos(\beta_\nu h)\sin(\beta_n z)\}$$

$$+\sum_{n=1}^{\infty} B_n\left\{-\frac{2}{(\alpha_n a)}\frac{\partial K_2(\alpha_n a)}{\partial(\alpha_n a)}+\frac{2}{(\alpha_n a)^2}K_2(\alpha_n a)\right\}\cos(\alpha_n h)\cos(\alpha_n z)$$

$$+\frac{\sigma_0}{G}\left\{1-\frac{3\nu}{1+\nu}\left(\frac{z}{a}\right)^2\right\}+C, \tag{62}$$

which in view of Eq. (58), finally leads to

$$\sigma_{\theta\theta}|_{\substack{r=a\\ \theta=\pi/2}}=[\sigma_{\theta\theta}^{(c)}+\sigma_{\theta\theta}^{(P)}]_{\substack{r=a\\ \theta=\pi/2}}=-\frac{2G}{1-2\nu}\sum_{\nu=1}^{\infty} A_\nu K_2(\beta_\nu a)$$

$$\times\{2(1+\nu)\cos(\beta_\nu h)\cos(\beta_\nu z)+\beta_\nu h\sin(\beta_\nu h)\cos(\beta_\nu z)-\beta_\nu z\cos(\beta_\nu h)\sin(\beta_n z)\}+3\sigma_0. \tag{63}$$

As a practical matter, Eq. (63) describes the behavior of the stress concentration factor through the thickness of the plate. It would be interesting at this point to see what happens to Eq. (63) as the Poisson's ratio $\nu \to 0$. From Eqs. (58–60), it becomes clear that

$$A_\nu \sim \frac{\nu}{1+\nu} \tag{64}$$

from which one may now easily deduce that

$$\lim_{\nu \to 0} \sigma_{\theta\theta}(a, \pi/2, z) = 3\sigma_0. \tag{65}$$

This result is in agreement with our expectations for it represents the result of an exact solution. It is also of interest to note that

$$\sigma_{\theta\theta}(a, 0, z) = -\sigma_{\theta\theta}(a, \pi/2, z) + 2\sigma_0, \tag{66}$$

which shows the point $(a, 0, z)$ to be in a state of compression, a result that clearly meets our physical expectations.

5 The stress concentration factor

Without going into the mathematical details, the system was solved numerically[8] and the stress concentration factor at $\theta = \pi/2$ and $r = a$ was computed for various radius to thickness ratios, a/h, and for Poisson's ratio of $\nu = 0.33$. The results are presented in Figs. 6–9. It may be noted that double precision was used throughout the numerical work and that a very sophisticated algorithm was used for the evaluation of the modified Bessel functions of the second kind.

The results show the stress concentration factor to be sensitive to the ratio of (a/h) and to Poisson's ratio ν. For example, for $\nu = 0.33$ and ratios of $(a/h) > 0.5$ it is found that the stress concentration factor attains its maximum in the middle of the plate and decreases parabolically as one approaches the free surfaces. On the other hand, for $(a/h) < 0.5$ the stress concentration factor attains its maximum close to the plate faces. Moreover, as the ratio of a/h decreases further, the following numerical trends are observed for the stress concentration factor (s.c.f.): (a) the magnitude of the rise slowly increases[9], (b) the maximum occurs closer and closer to the free surface (approximately a distance a away from the free surface), (c) at the surface of the plate it drops rather abruptly, (d) the magnitude at the surface slowly decreases.

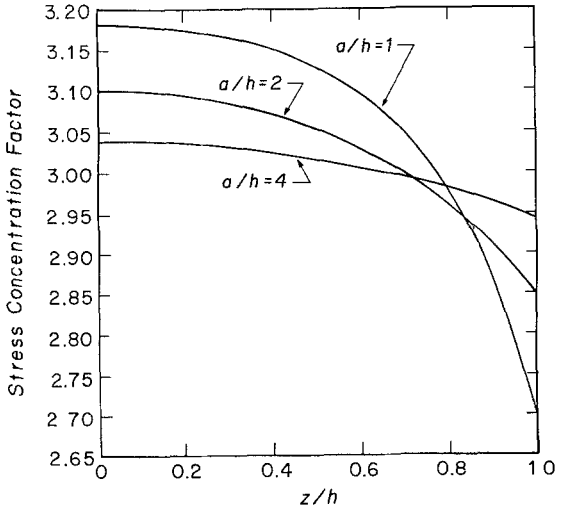

Fig. 6. Stress concentration factor across the thickness for Poisson's ratio $\nu = 0.33$ and various a/h ratios

[8] It should be noted that we have also constructed the orthogonality condition of these eigenfunctions

[9] The reader should be cautioned that this remark does not necessarily imply that the s.c.f. will increase indefinitely

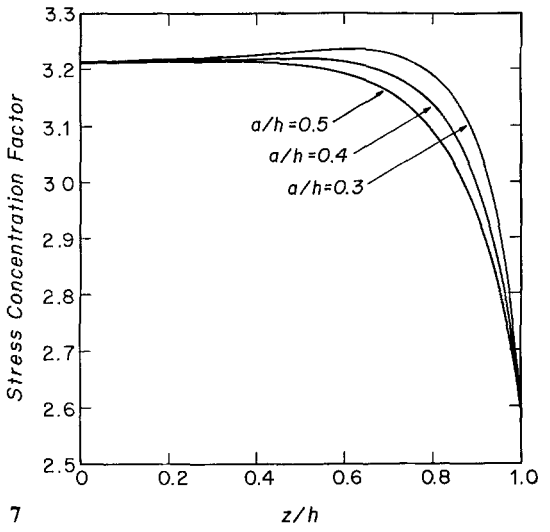

7

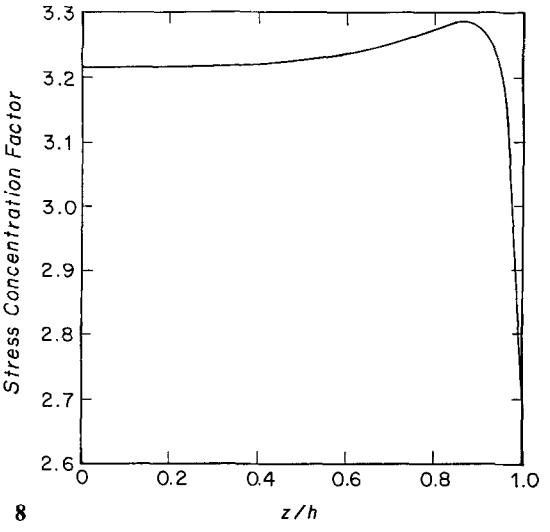

8

Figs. 7 and 8. Stress concentration factor across the thickness for Poisson's ratio of $\nu = 0.33$ and **7** various a/h ratios; **8** $a/h = 0.1$

We next compare our results with those already existing in the literature. For ratios $\nu = 1/4$ and $(a/h) > 1$ our results[10] are identical to those obtained by Alblas (1957). Moreover, for the ratio of $(a/h) = 1$ the difference is minimal as can be seen by the comparison of the results in Fig. 10. The small difference is attributed to the fact that Alblas at that time did not have access to modern day computer facilities, consequently, he was forced to truncate the system to fourteen roots. Our results on the other hand, reflect the use over 300 roots. Even so, the agreement for ratios of $(a/h) \geqq 1$ is remarkably good. For ratios of $(a/h) < 1$, however, many more roots are necessary in order to eliminate undesirable oscillations and as a result the authors believe that Alblas was forced to limit his calculation to ratios of $(a/h) \geqq 0.5$. Be that as it may, Alblas leaves the reader with the impression that the s.c.f. always decreases as one approaches the free surfaces of the plate.

Our present results substantiate the existence of a boundary layer at the vicinity of the free surfaces. In fact, if we examine the local behavior of the rise, e.g., for the ratio of $(a/h) = 0.01$, and stretch the variable, by letting $\xi = 100\,(1 - z/h)$, we observe (Fig. 11) that the behavior is similar to[11] that obtained by Youngdahl and Sternberg (1966). We also observe that the rise here is not quite as noticeable as it is in Fig. 9. This is due to the vertical scale which Youngdahl and Sternberg (1966) used and due to the stretching of the horizontal variable z/h. In view of the findings of Youngdahl and Sternberg (1966), one concludes that the surface effects become dominant and the amplitude of the characteristic rise ultimately reaches an upper bound.[12]

Finally, taking into account the loading in Youngdahl and Sternberg (1966) and using our present results for $a/h = 0.05$ together with the principle of superposition, we calculate the displacement function w at $z = h$. A comparison of these results with those of Youngdahl and Sternberg (1966) shows a very good agreement as can be seen in Fig. 12.

Perhaps it is appropriate to point out an interesting observation made by Youngdahl and Sternberg (1966) "..., the burden of the numerical analysis of the solution established was at least equal to the effort expended on its derivation".

The present authors also concur with this observation for the nature of this problem is such that it does not lend itself to routine numerical calculations.

Finally it is appropriate to comment on the conditions of plane stress and plane strain. For $(a/h) \to \infty$, our numerical results give precisely the value of plane stress, i.e. the value of 3. In the

---

[10] Alblas computed the s.c.f. for $a/h \geqq 0.5$ and for $\nu = 1/4$ only

[11] In Youngdahl and Sternberg (1966), the reader should notice that the loading is in both the x and the y directions

[12] For $a/h = 0.01$ and $\nu = 0.33$, our numerical results show the max. value of the s.c.f. to be 3.3675. The value should be very close to the upper bound. It is interesting to note that it is $\approx 3/(1 - \nu^2)$

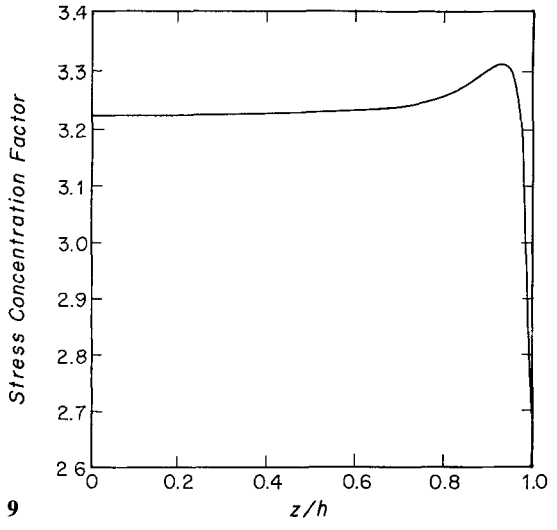

9

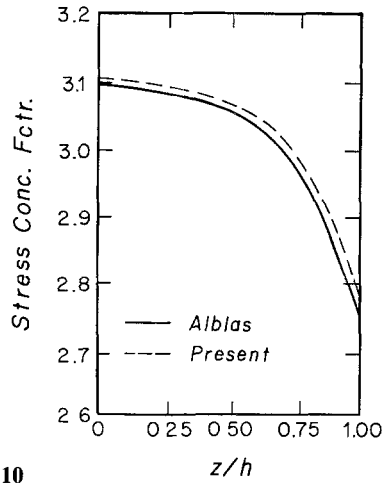

10

Figs. 9 and 10. **9** Stress concentration factor across the thickness for Poisson's ratio of $\nu = 0.33$ and $a/h = 0.05$. **10** Comparison of the stress concentration factor for $\nu = 0.25$ and $a/h = 1.0$

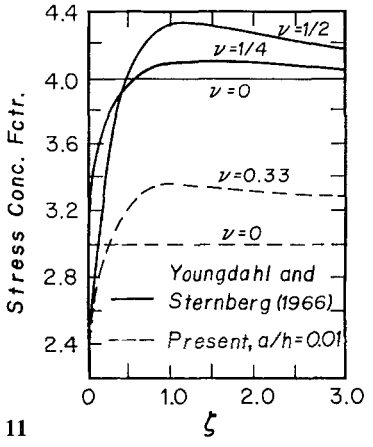

11

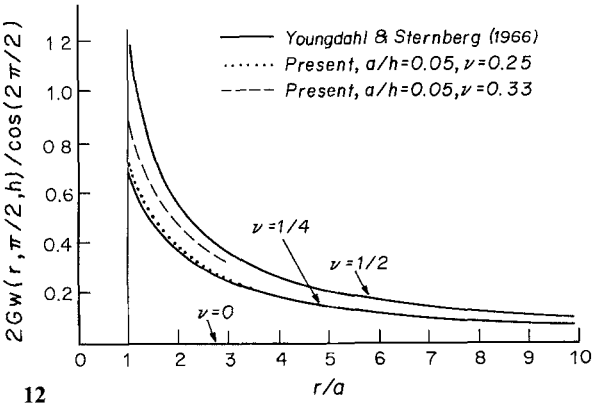

12

Figs. 11 and 12. Comparison **11** of the stress concentration factor in the vicinity of the free surface with results of (Youngdahl and Sternberg 1966); **12** of the displacement w at $z = h$ with the results of Youngdahl and Sternberg (1966)

case of plane strain, the boundary planes $z = \pm h$ are thrown to infinity and simultaneously the boundary conditions must be relaxed by requiring that all stresses and displacements must be finite. Assuming that the radius of the hole is sufficiently large, the author suspects that the s.c.f. at the center of the plate will begin to slowly decrease, as the ratio of (a/h) decreases beyond the value of 0.05, until it finally reaches the value of plane strain. To establish this, however, would require considerable more computer time and this was not available to us.

6 The stress behavior at the corner

Finally, it is of some academic and practical interest to examine the behavior of the stress field in the very immediate vicinity of the corner point, i.e., the point where the hole meets the free surface of the plate. Such information, however, is best if it is extracted by analytical rather than numerical

means. Utilizing the local coordinates of the corner point, an asymptotic analysis[13] was carried out for the exponent α of an assumed displacement field $u_i \sim \rho^\alpha$, where $\rho \ll a$ and $r = a + \rho \cos \phi$, $z = h - \rho \sin \phi$. Without going into the mathematical details, the satisfaction of all the boundary conditions of the $3D$ stress problem lead to a characteristic equation which has an infinite number of complex roots. It is interesting to note that the first root is the same as that obtained by the Williams solution (Williams 1952) for a 90° corner with free–free stress boundaries, i.e., $\alpha = 2.73959 \pm i\,1.11902$. While this result was to be anticipated on intuitive grounds, it could not be taken for granted.

Returning next to the footnote number 7, we observe that the numerical results show all three Eqs. (58–60) to be satisfied for all values of z, including the end points. Moreover, the asymptotic analysis for $\rho \ll a$ clearly shows that no stress singularity is present at the corner.

7 Conclusions

Despite careful detail-design, practically any structure contains stress concentrations due to holes. Bolt holes and rivet holes are necessary components for structural joints, e.g., connection holes for pipes, access holes etc. It is not surprising, therefore, that the majority of service cracks nulceate in the area of stress concentration at the edge of a hole. The subject of eventual concern, therefore, is the use of the principles of modern fracture mechanics for the derivation of appropriate and reliable design criteria that will insure the structural integrity of the joints. In deriving such criteria a knowledge of the three-dimensional stress concentration factor is a prerequisite.

The present analysis describes the effect which specimen thickness has on the stress concentration factor and suggests the following conclusions:

The solution is derivable from a general $3D$ solution to Navier's equations; the solution recovers the existing limiting results for thin plates (Alblas 1957; Reiss 1963) as well as for thick plates (Youngdahl and Sternberg 1966) and bridges the gap in between; for ratios of $(a/h) > 0.5$, the maximum stress occurs at the middle plane; for ratios of $(a/h) < 0.5$, the maximum stress occurs close to the free surface (approximately one radius distance away from the surface); the results offer a definition of what is considered to be a thin or a thick plate this (depends on ν and a/h); as (a/h) becomes small there exists in the neighborhood of the free surfaces a boundary layer solution similar to that reported in Youngdahl and Sternberg (1966); depending on the value of the ratio of a/h, the fatigue life of the structure may be substantially shorter than that predicted by the $2D$ elasticity theory; for $\rho \ll a$ there is no stress singularity present at the corner where the hole meets the free surface of the plate.

Acknowledgments

The contents of this paper represent an outgrowth of some previous work on $3D$ Fracture which was supported by AFOSR. The author is grateful for this support.

References

Alblas, J. B. (1957): Theorie van de driedimensionale spanningstoestand in een doorboovde plaat. Dissertation, Technische Hogeschool Delft, H. J. Pairs, Amsterdam

Broek, D. (1974): Elementary engineering fracture mechanics. In: Chapt. 14: Plates with holes, 4th edn., pp. 361–370. Groningen: Nordhoff

Folias, E. S. (1975): On the three-dimensional theory of cracked plates. J. Appl. Mech. 42, 663–674

Folias, E. S. (1987): The 3D stress field at the intersection of a hole and a free surface. Int. J. Fracture 35, 187–194

Green, A. E. (1948): Three-dimensional stress system in isotropic plates, I. Trans. R. Soc. London, Ser. A. 240.285 561

[13] The details of this asymptotic analysis are reported in Folias (1986)

Green, A. E. (1949): The elastic equilibrium of isotropic plates and cylinders. Proc. R. Soc. London, Ser. A. 195, 533
Kantorovich, L. V.; Krylov, V. I. (1964): Approximate methods of higher analysis. Groninger: Nordhoff
Kirsch, G. (1898): Die Theorie der Elastizitat and die Bedürfnisse der Festigkeitslehre. Z. Vereines Deutscher Ing. 42, 797–807
Muskhelishvili, N. I. (1953): Some basic problems of mathematical theory of elasticity. Groningen: Nordhoff
Neuber, H. (1985): Kerbspannungslehre. Berlin, Heidelberg, New York: Springer
Reiss, E. L. (1963): Extension of an infinite plate with a circular hole. J. Soc. Ind. Appl. Math. 11, 840
Savin, G. N. (1961): Stress concentration around holes. New York: Pergamon Press
Sternberg, E.; Sadowsky, M. A. (1949): Three dimensional solution of the stress concentration around a circular hole in a plate of arbitrary thickness. J. Appl. Mech. 16, 27–38
Wilcox, C. H. (1978): Completeness of the eigenfunctions for Griffith cracks in plates of finite thickness. Interim report, Dept. of Mathematics, University of Utah
Wilcox, C. H. (1979): Uniqueness theorems for displacement fields with locally finite energy in linear elastostatics. J. Elasticity, 9, 221–243
Williams, M. L. (1952): Stress singularities resulting from various boundary conditions in angular corners of plates in extension. J. Appl. Mech. 19, 526
Youngdahl, C. K.; Sternberg, E. (1966): Three-dimensional stress concentration around a cylindrical hole in a semi-infinite elastic body. J. Appl. Mech. 33, 855

Communicated by S. N. Atluri, April 1, 1989